The Astrophysical Journal, 664:448–457, 2007 July 20

THE POST-BURST AWAKENING OF THE ANOMALOUS X-RAY PULSAR IN WESTERLUND 1

G. L. Israel,[1] S. Campana,[2] S. Dall'Osso,[1] M. P. Muno,[3] J. Cummings,[4] R. Perna,[5] and L. Stella[1]

Received 2006 November 20; accepted 2007 March 15

ABSTRACT

On 2006 September 21, an intense ($\sim 10^{39}$ erg s^{-1}) and short (20 ms) burst was detected by *Swift* BAT at a position consistent with that of the candidate anomalous X-ray pulsar (AXP) CXOU J164710.2−455216, discovered by *Chandra* in 2005. *Swift* follow-up observations began ∼13 hr after the event and found the source at a 1–10 keV flux level of about 4.5×10^{-11} erg cm^{-2} s^{-1}, i.e., ∼300 times brighter than measured 5 days earlier by *XMM-Newton*. We report the results obtained from *Swift* BAT observations of the burst and subsequent *Swift* XRT observations carried out during the first 4 months after the burst. These data are complemented with those from two *XMM-Newton* observations (carried out just before and after the BAT event) and four archival *Chandra* observations carried out between 2005 and 2007. We find a phase-coherent solution for the source pulsations after the burst. The evolution of the pulse phase comprises an exponential component decaying with timescale of 1.4 days, which we interpret as the recovery stage following a large glitch ($\Delta\nu/\nu \sim 6 \times 10^{-5}$). We also detect a quadratic component corresponding to a spin-down rate of $\dot{P} \sim 9 \times 10^{-13}$ s s^{-1}, implying a magnetic field strength of 10^{14} G. During the first *Swift* XRT observation taken 0.6 days after the burst, the spectrum showed a $kT \sim 0.65$ keV blackbody ($R_{\rm BB} \sim 1.5$ km) plus a $\Gamma \sim 2.3$ power law accounting for about 60% of the 1–10 keV observed flux. Analysis of *Chandra* archival data, taken during 2005 when the source was in quiescence, reveal that the modulation in quiescence is 100% pulsed at energies above ∼4 keV and consistent with the (unusually small-sized) blackbody component being occulted by the neutron star as it rotates. These findings demonstrate that CXOU J164710.2−455216 is indeed an AXP; we compare them with the properties of three other AXPs which displayed similar behavior in the past.

Subject headings: pulsars: individual (CXOU J164710.2−455216) — stars: neutron — X-rays: bursts

1. INTRODUCTION

In recent years there has been a large observational and theoretical effort aimed at unveiling the nature of a sample of peculiar high-energy pulsars, namely the anomalous X-ray pulsars (AXPs; eight objects plus one candidate) and the soft γ-ray repeaters (SGRs; four objects plus three candidates). SGRs were discovered in the 1970s through the very intense bursts that they sporadically emit in the soft γ-ray band; AXPs were recognized as a distinct class of X-ray pulsars only a decade ago by virtue of their peculiar persistent emission and spin-down properties in the X-ray band (Paczyński 1992; Mereghetti & Stella 1995; for a recent review see Woods & Thompson 2004). It is now commonly believed that AXPs and SGRs are linked at some level, owing to their similar timing properties (spin periods in the 5–12 s range and period derivatives $\dot{P}$ in the 10^{-11} to 10^{-13} s s^{-1} range). Both classes have been proposed to host neutron stars whose emission is powered by the decay of their extremely strong inner magnetic fields (>10^{15} G; Duncan & Thompson 1992; Thompson & Duncan 1995). The detection of X-ray bursts from 1E 1048.1−5937, 1E 2259+586, 4U 0142+614, and XTE J1810−197 has strengthened the possible connection between AXPs and SGRs (Gavriil et al. 2002; Kaspi et al. 2003, 2006; Woods et al. 2005), as well as the magnetar scenario.

Different types of X-ray flux variability have been displayed by AXPs, including slow and moderate flux changes (up to a factor of a few) on timescales of years (virtually all the objects of the class), moderately intense outbursts (flux variations of a factor up to 10) lasting for 1–3 yr (1E 2259+586, and 1E 1048.1−5937), and dramatic and intense SGR-like burst activity (fluence of 10^{36}–10^{37} erg) on subsecond timescales (4U 0142+614, XTE J1810−197, 1E 2259+586 and 1E 1048.1−5937; see Kaspi 2006 for a recent review on the X-ray variability). Particularly important was the 2002 bursting/outbursting event detected from 1E 2259+586, the only known event in which a factor of ∼10 persistent flux enhancement in an AXP was detected in coincidence with a burst-active phase during which the source displayed more than 80 short bursts (Gavriil et al. 2004; Woods et al. 2004). The timing and spectral properties of the sources changed significantly during this phase and recovered within a few days. The short recovery time is likely because of the relatively high X-ray luminosity level of the pre-outburst phase ($\sim 10^{35}$ erg s^{-1} in the 1–10 keV band). In 2003 the first transient AXP, XTE J1810−197, was discovered. This source displayed a factor of ∼100 persistent flux enhancement with respect to the pre-outburst quiescent luminosity level ($\sim 10^{33}$ erg s^{-1}), where no pulsations were detected. Unfortunately, since the initial phases of the outburst were missed, we do not know whether an active bursting phase set in, similar to that of 1E 2259+586, in this source also, leaving several questions concerning the mechanisms of the outburst onset unanswered (Ibrahim et al. 2004; Gotthelf et al. 2004; Israel et al. 2004; Rea et al. 2004). Until now, no transient bursting-outbursting AXP was known.

On 2006 September 21, a burst was detected by the *Swift* Burst Alert Telescope (BAT) at a position consistent with the AXP candidate CXOU J164710.2−455216 in the open cluster Westerlund 1 (Krimm et al. 2006; Muno et al. 2006b). The 20 ms duration of the burst suggested that the origin of the burst was indeed the candidate AXP. Unfortunately, since the burst was initially attributed

[1] INAF-Osservatorio Astronomico di Roma, Via Frascati 33, I-00040 Monteporzio Catone, Roma, Italy; gianluca@mporzio.astro.it, stella@mporzio.astro.it.
[2] INAF-Osservatorio Astronomico di Brera, Via Bianchi 46, I-23807 Merate, Lc, Italy.
[3] Space Radiation Laboratory, California Institute of Technology, Pasadena, CA 91125.
[4] University of Maryland, Baltimore County/NASA Goddard Space Flight Center, Greenbelt, MD 20771.
[5] JILA, University of Colorado, Boulder, CO 80309-0440.

TABLE 1
Swift Observation Log for CXOU J164710.2−455216

Sequence ID	Instrument/Mode	Start Time (TDB)	End Time (TDB)	Exposure (s)
00230341000[a]	BAT/EVENT	2006 Sep 21, 01:34:11	2006 Sep 21, 01:34:54	43
00030806001.....	XRT/WT	2006 Sep21, 14:29:13	2006 Sep 21, 22:10:33	1919.9
00030806001.....	XRT/PC	2006 Sep 21, 14:29:29	2006 Sep 21, 22:27:44	7736.6
00030806002.....	XRT/WT	2006 Sep 22, 14:38:22	2006 Sep 22, 14:51:10	766.9
00030806003.....	XRT/WT	2006 Sep 22, 19:39:09	2006 Sep 23, 05:04:12	4910.0
00030806003.....	XRT/PC	2006 Sep 22, 19:39:17	2006 Sep 23, 01:44:13	1765.6
00030806004.....	XRT/WT	2006 Sep 26, 06:36:51	2006 Sep 26, 11:35:03	1250.0
00030806004.....	XRT/PC	2006 Sep 26, 08:12:58	2006 Sep 26, 11:42:46	2482.3
00030806006.....	XRT/WT	2006 Oct 02, 11:04:54	2006 Oct 02, 17:09:01	1977.6
00030806007.....	XRT/WT	2006 Oct 03, 12:19:42	2006 Oct 03, 14:12:54	2034.1
00030806008.....	XRT/WT	2006 Oct 05, 23:59:24	2006 Oct 06, 01:48:39	2158.9
00030806009.....	XRT/WT	2006 Oct 09, 17:51:53	2006 Oct 09, 22:51:11	3521.8
00030806010.....	XRT/WT	2006 Oct 10, 00:09:50	2006 Oct 10, 02:13:09	2829.4
00030806011.....	XRT/WT	2006 Oct 15, 05:38:04	2006 Oct 15, 12:21:36	5617.9
00030806012.....	XRT/WT	2006 Oct 21, 02:56:44	2006 Oct 21, 08:07:58	5508.0
00030806013.....	XRT/WT	2006 Oct 27, 16:10:55	2006 Oct 27, 19:42:44	2816.6
00030806014.....	XRT/WT	2007 Jan 19, 04:05:59	2007 Jan 19, 06:00:28	2051.8
00030806015.....	XRT/WT	2007 Jan 22, 01:07:57	2007 Jan 22, 04:44:42	3817.7

[a] BAT trigger.

to a nearby Galactic source, the burst BAT position was not promptly re-observed by *Swift*. Moreover, because of the relatively low significance of the burst detection, the event was initially tagged as "not real." A subsequent careful analysis of the data confirmed that the detection was indeed real (Krimm et al. 2006). We activated a Target of Opportunity (ToO) observation program with *Swift* in order to look for burst-induced persistent flux variations of the source. The first *Swift* pointing was carried out 13 hr after the burst. The AXP was detected at a flux level about 300 times higher than that in the previous measurement (5 days before, from an *XMM-Newton* Guest Observer Program pointing; Muno et al. 2006a; 1–10 keV flux level of $\sim 1.5 \times 10^{-13}$ erg cm^{-2} s^{-1}), hence confirming the transient behavior of CXOU J164710.2−455216 (Campana & Israel 2006; Israel & Campana 2006; Ibrahim et al. 2004).

A first radio observation of CXOU J164710.2−455216 was carried out from Parkes at 1.4 GHz a week after the outburst onset, with the goal of searching for pulsed emission similar to the case of XTE J1810−197 (Camilo et al. 2006). The data put a tight upper limit of 40 μJy on the presence of pulsed emission from the source (Burgay et al. 2006). The position of CXOU J164710.2−455216 was also observed serendipitously by IBIS/ISGRI on board *INTEGRAL* on 2006 September 22 (23 ks of effective exposure time): the source was not detected and 3 σ upper limits of 5×10^{-11} erg cm^{-2} s^{-1} in the 20–40 keV band and 1.7×10^{-10} erg cm^{-2} s^{-1} in the 40–200 keV band were derived (Götz et al. 2006). Near-IR observations were carried out on 2006 September 29 in the K_s band and reaching a limiting magnitude of 20.3 (3 σ; Wang et al. 2006): no IR counterpart or variable object was found at the *Chandra* position of CXOU J164710.2−455216.

In this paper we report the results from the initial *Swift* BAT detection and the subsequent *Swift* XRT monitoring campaign consisting of 15 ToO observations. We also report on a re-analysis of archival *Chandra* data sets of Westerlund 1, which allowed us to carry out the first pulse-phase spectroscopic study of CXOU J164710.2−455216 in quiescence. Finally, we compare the observed behavior of CXOU J164710.2−455216 with that of three other AXPs (XTE J1810−197, 1E 1048.1−5937 and 1E 2259+586), which displayed a similar phenomenology in the past.

2. OBSERVATIONS AND RESULTS

The *Swift* data (see Table 1) were reduced with the standard BAT and XRT analysis software distributed within HEAsoft (ver. 6.0.5) to produce cleaned event lists. For the XRT data we considered Windowed Timing (WT) and Photon Counting (PC) mode data (see Hill et al. 2004 for a full description of read-out modes) and further selected XRT grades 0–12 and 0–2 for WT and PC data, respectively (according to *Swift* nomenclature; Hill et al. 2004). XMMSAS version 20060628_1801-7.0 and CIAO version 3.3.0.1 were used to reduce the *XMM-Newton* and *Chandra* data, respectively. Timing and spectral analyses were carried out with XSPEC version 12.2.1, Xronos version 5.21, and ad hoc developed pipelines (Israel & Stella 1996; Dall'Osso et al. 2003).

2.1. *The BAT Event*

The BAT event took place at 01:34:52 in Barycentric Dynamical Time (TDB) on 2006 September 21. It was the first burst ever detected from an AXP at energies above 20–30 keV. We analyzed the $\sim$20 ms integrated spectrum by considering the data in the 15–150 keV energy range and applying an energy-dependent systematic error vector.[6] Owing to poor statistics, a preferred model could not be singled out: both a blackbody and a power-law component gave $\chi^2_\nu \approx 1$ (3 degrees of freedom, hereafter dof; see Fig. 1). A kT of $9.9^{+2.8}_{-2.2}$ keV and a Γ of 1.8(5) were obtained for the two models (errors are at 90% confidence level). In both cases a fluence was found of $\approx 10^{-8}$ erg cm^{-2}, corresponding to a total energy of $\sim 2 \times 10^{37}$ erg (for an assumed distance of 5 kpc). Assuming an exponential decay for the burst flux, we determined a decay time τ of 3(1) ms (1 σ confidence level) from the 5 ms binned BAT light curve centered around the trigger (Fig. 1, *inset*). Compared with the properties of previously detected AXP bursts, the event from CXOU J164710.2−455216 had a duration within 1 σ of the lognormal distribution average value inferred for 1E 2259+586,

[6] See http://www.heasarc.gsfc.nasa.gov/docs/swift/analysis/bat_digest.html.

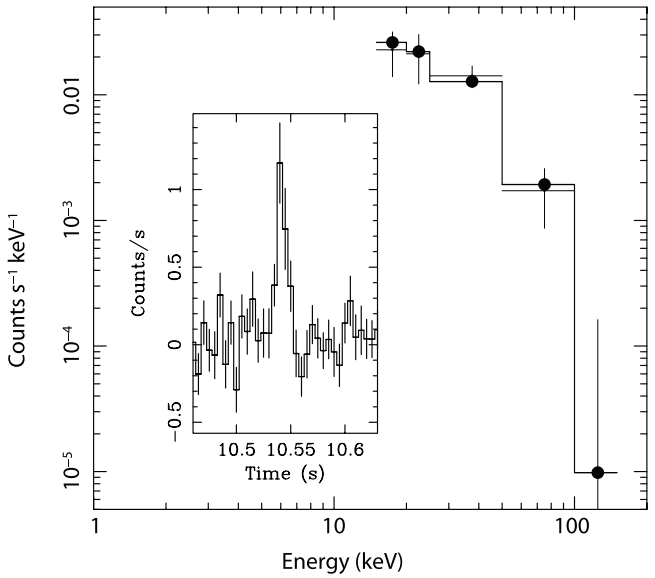

FIG. 1.—The 15–150 keV *Swift* BAT spectrum of the 20 ms long burst detected from CXOU J164710.2−455216 on 2006 September 21, together with the 5 ms binned BAT light curve in the time interval around the trigger (*inset*).

while the fluence is significantly larger (by a factor of ∼50) than the mean (Gavriil et al. 2004). Out of ∼80 detected from 1E 2259+586, only three had fluences comparable to or slightly larger than that of the BAT event, while only one of the three shared a comparable duration.

2.2. *XRT Monitoring Observations*

Swift observed CXOU J164710.2−455216 on 15 epochs between the BAT event and 2007 January 22, for a total effective exposure time of ∼50 ks (see Table 1). For the WT mode data, the extraction region was computed automatically by the analysis software and was a rectangle of 40 pixels along the WT strip, centered on the source and encompassing ∼98% of the point-spread function in this observing mode. For PC mode observations, data were extracted from a circle with 30 pixel radius centered on the source. Background spectra were taken in PC mode from annular regions (inner and outer radii of 70 and 90 pixels, respectively), and in WT mode from a 40 pixel rectangular region in the vicinity of the source and free of sources. The photon arrival times were corrected to the solar system barycenter. Note that the absolute timing calibration of the XRT is ≈200–300 μs (Cusumano et al. 2005). Spectra were extracted from the same event lists. The 1–10 keV band was used in the spectral fitting. Spectra were rebinned so as to have at least 20 counts per energy bin, so that minimum χ^2 techniques could be reliably used in the fitting.

2.2.1. *Spectral Analysis*

We fitted the 1–10 keV band spectral data from the first *Swift* ToO observation of CXOU J164710.2−455216 with the pre-outburst models reported in literature (Muno et al. 2006b; Skinner et al. 2006). The single absorbed blackbody (BB) model did not give acceptable results (reduced χ^2 of 1.3 for 225 dof). A better fit (reduced $\chi^2 \sim 1.0$ for 223 dof) was obtained by using an absorbed BB with $kT = 0.63(4)$ keV, $R_{\rm BB} = 2.1(1)$ km at 5 kpc, plus a power-law (PL) component with photon index $\Gamma = 2.3(2)$ (see Fig. 2). $N_{\rm H}$ was fixed at the pre-outburst value of 1.9×10^{22} cm^{-2} measured with *Chandra*. Alternatively, two BBs with $kT_s = 0.50(5)$ keV [$R_{{\rm BB}s} = 3.2(4)$ km] and $kT_h = 1.1^{+0.2}_{-0.1}$ keV [$R_{{\rm BB}h} = 0.5(1)$ km; all the uncertainties are at the 90% level; Campana & Israel 2006; Israel & Campana 2006]. An *F*-test showed that the inclusion of the second component is significant at the 7 σ level. The 1–10 keV observed and unabsorbed fluxes were 3.7×10^{-11} erg cm^{-2} s^{-1} and 8.4×10^{-10} erg cm^{-2} s^{-1}, respectively, for both the two-BB and the BB-plus-PL models (the PL component accounts for up to about 60% of the observed flux). We note that the parameters of the BB component in the BB-plus-PL model are significantly different from those inferred in quiescence ($kT_s = 0.50$ keV and $R_{\rm BB} = 0.36$ km; Skinner et al. 2006; see also § 2.3).

In the following analyses we adopt the canonical BB-plus-PL component to fit the entire *Swift* data set (although there are no statistical reasons to prefer this model over the two-BB model). We first fitted all together the spectra obtained in 2006, by leaving all model parameters free except for $N_{\rm H}$, which we kept fixed at the value determined by *Chandra* (see above). The values of kT and Γ were both consistent with being constant in time with marginal evidence of Γ becoming steeper as the outburst evolved. Therefore, we fixed both the BB temperature and the PL photon index to the values inferred from the first *Swift* pointing (which has largest S/N) and fitted all spectra together again. The PL dominated the CXOU J164710.2−455216 flux during the first 10 days from the burst. The BB component accounted for nearly 80%–90% of the total flux during the *Swift* observations one month later; this was similar to the spectrum in quiescence where the PL component was only marginally detectable (see also § 2.3). During the latest *Swift* observation on 2007 January, the source was caught at a 1–10 keV observed flux level of 7.8×10^{-12} erg cm^{-2} s^{-1}, and only the BB component was detected with a characteristic temperature of $kT = 0.61(3)$ keV and radius $R_{\rm BB} = 1.7(1)$ km, clearly suggesting a cooling of the BB component as the size of the emitting region increases.

2.2.2. *Timing*

In this analysis we also included data from two *XMM-Newton* and two *Chandra* observations.[7] We started by inferring an accurate period measurement by folding the data from each observation at the period reported by Muno et al. (2006b; see also § 2.3). The majority of the resulting pulse profiles had three different peaks.

The relative phases and amplitudes were such that the signal phase evolution could be followed unambiguously for the observations in the 2006 October 2–27 time interval (see Fig. 3). The resulting phase-coherent solution had a best-fit period of $P = 10.610652(1)$ s (uncertainties here are 1 σ). TJD 13999.0 was used as reference epoch; details on the phase-fitting technique are given in Dall'Osso et al. (2003). A quadratic component was required at 4 σ confidence level in the phase residual versus time fit. This corresponds to $\dot{P} = 2.4(6) \times 10^{-12}$ s s^{-1}. The value of $\dot{P}$ is consistent, at the 2 σ level, with the measurement of $\dot{P} \simeq 1.55(50) \times 10^{-12}$ s s^{-1} reported by Woods et al. (2006), who considered the data from 4 *Chandra* observations (from 2006 September 27 to October 28) in their fitting, and with the upper limit of $\sim 5.6 \times 10^{-12}$ s s^{-1} derived by Israel et al. (2006) based on a reduced data sample.

Next, we compared our phase-coherent pulse profile with that derived from observations carried out in the 2006 September 21–26 time interval. The signal shape showed large changes across different observations. A one-to-one correspondence between peaks in different observations was found based on the fact that the

[7] For the reduction of the two *XMM-Newton* observations we refer to Muno et al. (2007); for the *Chandra* data reduction and analysis (obtained in continuous clock CC33_FAINT mode) we refer to the procedure reported, as an example, in Rea et al. (2005).

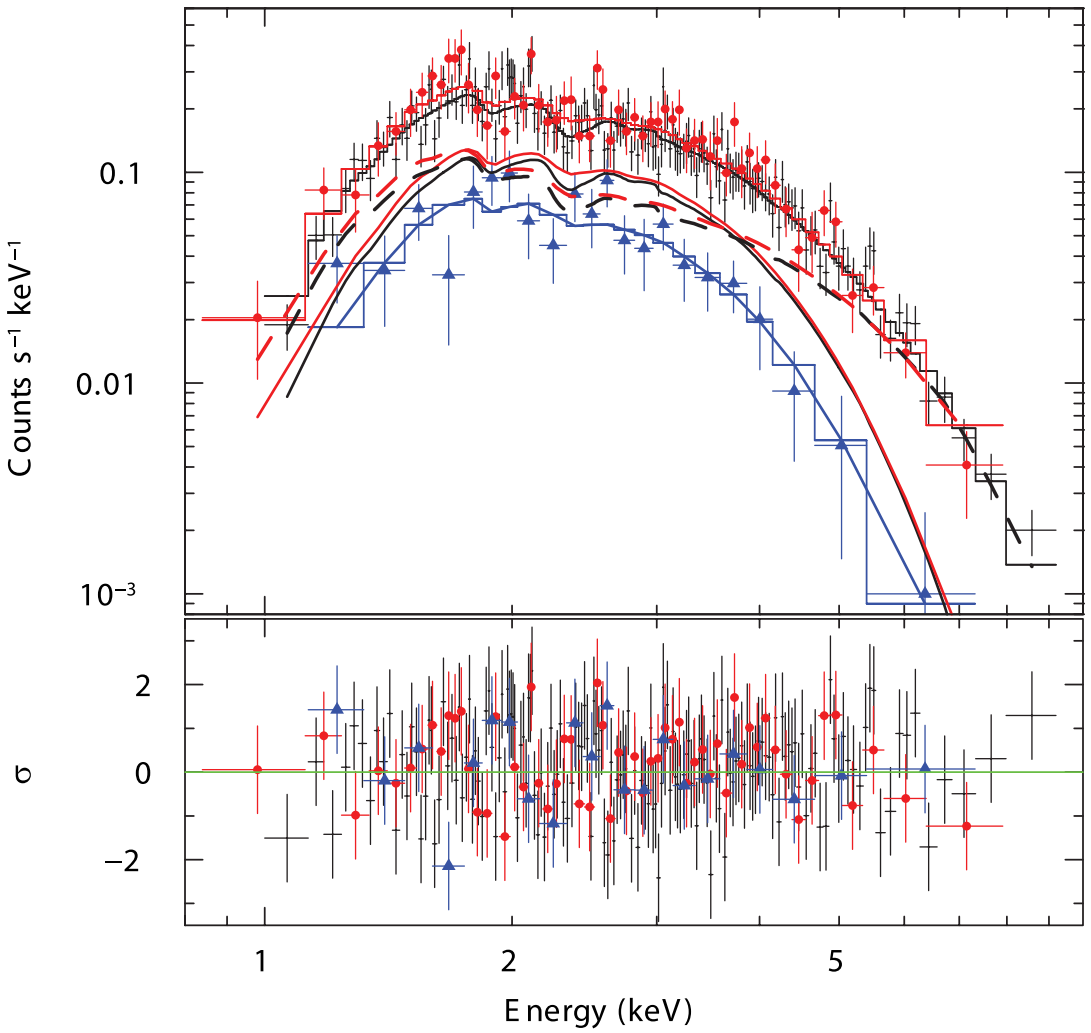

FIG. 2.—The 1–10 keV *Swift* XRT spectra obtained during the first ToO observation started 13 hr after the BAT event (2006 September 21), and the most recent one started 120 days later (2007 January 19–22; *filled triangles*) are shown together with the model residuals. Both the WT (*filled circles*) and PC mode spectra are displayed for the first observation and fitted with the BB-plus-PL (*solid and dashed lines, respectively*) model discussed in the text. During the 2007 January observation (only WT mode data were obtained) the PL component was not present anymore.

reference/main peak and the dim peak remained nearly constant, both in amplitude and relative phase, during the whole observing period (see Fig. 3). The third peak was highly variable in amplitude, becoming comparable to, or even larger than, the reference peak after ~10 days from the BAT event. The correctness of the reference and dim peak identification was supported by the fact that at higher energies the shape of the postburst pulse profile a few days after the BAT event resembled more closely the single-peaked preburst pulse profile, as shown by Muno et al. (2007; see also Fig. 3). Based on the above findings, we were thus able to track the phase evolution of the reference/main peak back to the first *Swift* observation. We note that techniques based on the cross-correlation of folded light curves from different observations proved unreliable in our case, as they tended to favor the alignment of the highest peak in each observation.

The phase-coherent solution determined for the 2006 October 2–27 time interval could not be extrapolated backward to also fit the phases of the 2006 September 21–26 observations, not even by introducing higher period derivatives (up to the fourth order). The fit was improved by introducing an exponential term in the phase model, a likely signature of the occurrence of a pulsar glitch. The model consisting of an exponential plus a linear and quadratic term gave a $\chi^2 = 4.7$ for 5 dof. In our best-fit model, the exponential component has an *e*-folding time of $\tau = 1.3(1)$ days and an amplitude of $\Delta\nu = 1.0(1) \times 10^{-5}$ Hz. These parameters imply a large glitch, with $\Delta\nu/\nu \simeq 10^{-4}$.

Subsequently, we included three additional data sets obtained in 2007: two short *Swift* ToO observations carried out on 2007 January 19–22 at the beginning of the new visibility window of the source (see Table 2) and an archival *Chandra* DDT observation carried out on 2007 February 2. Unfortunately, the extrapolation of our phase-coherent solution (at 99% confidence level) to 2007 January 19–22 observations resulted in a one-cycle uncertainty, such that phase coherence was lost. The two possible phase values for the reference peak (separated by 2π) yielded two solutions (see Fig. 4). These are: (1) $P = 10.610655(1)$ s and $\dot{P} = 8.9(6) \times 10^{-13}$ s s^{-1}, and (2) $P = 10.610652(1)$ s and $\dot{P} = 2.4(6) \times 10^{-12}$ s s^{-1}. However, the expected phase shift for the two solutions in the ~2 week long gap between the first *Swift* observation and the latest *Chandra* pointing is about 0.1 for solution (1) and 0.3 for solution (2). This provides a way to solve the ambiguity, thus recovering phase coherence. Indeed, our phase-fitting analysis showed that the pulse phase shift accumulated is ~0.11(2), unambiguously identifying solution (1) as the correct one. Fitting the whole sample of phases with a linear (P), a quadratic ($\dot{P}$), and an exponential component (glitchlike event),

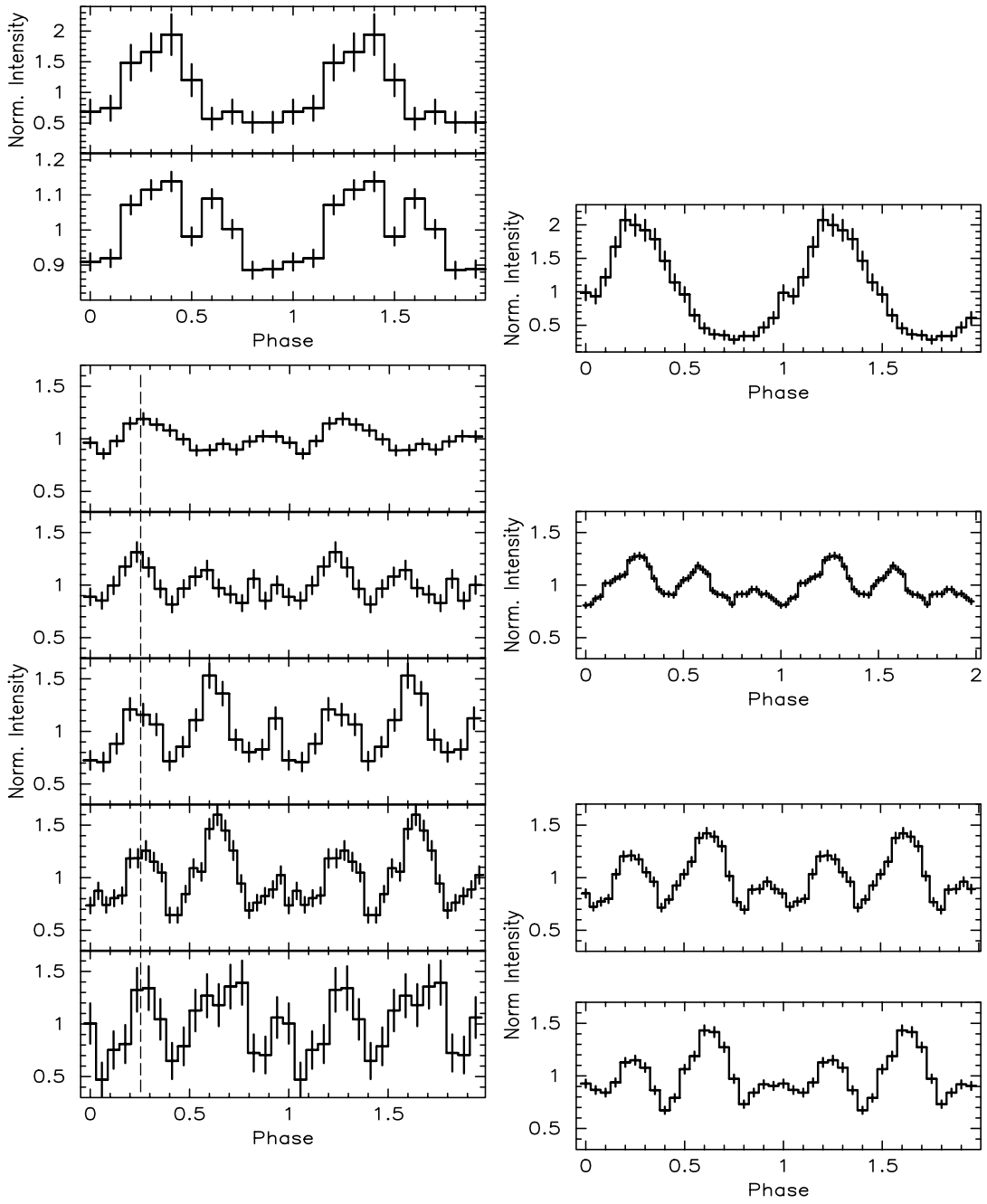

FIG. 3.—The 3.5–10 keV *XMM-Newton* PN light curves (*top left*; 5 days before and 2 days after the BAT event), the 1–10 keV *Swift* XRT light curves referring to $t_0 + 0.7$ days, $t_0 + 1.8$ days, $t_0 + 12$ days, $t_0 + [15;\ 37]$ days, and $t_0 + [120]$ days from top to bottom (*bottom left*). *Right*: The 1–10 keV *XMM-Newton* PN and *Chandra* ACIS-S light curves referring to $t_0 - 5$ days, $t_0 + 1.7$ days, $t_0 + 38$ days, and $t_0 + 135$ days folded by using the P-$\dot{P}$ coherent timing solution discussed in the text. The peak at phase ~0.25 marked by the stepped line represents our reference peak. The peak at phase ~0.6 is the highly variable component we identify.

we derived the following final solution: $P = 10.6106549(2)$ s, $\dot{P} = 9.2(4) \times 10^{-13}$ s s^{-1}, $\tau = 1.4(1)$ days and an amplitude $\Delta\nu = 6.1(3) \times 10^{-6}$ Hz, corresponding to a $\Delta\nu/\nu = 6.5(3) \times 10^{-5}$ (reduced χ^2 of 1 for 14 dof). We note that the periods inferred from the single pre- and postburst *XMM-Newton* observations (which have a sufficiently good statistics for phase-fitting techniques to be used) are $P = 10.61066(4)$ s and 10.61056(5) s, respectively, therefore implying a $\Delta P \sim 10^{-4}$ s. On the other hand, the expected ΔP at the second *XMM-Newton* observation epoch, as inferred from the exponential decay parameters, is $\sim 2 \times 10^{-4}$, which is in the same range as the ΔP reported above.

We also tried to include the phase point obtained from the first *XMM-Newton* observation, carried out ~5 days before the BAT event, in our solution for the postburst phase. We identified the single peak of the folded light curve as the reference peak we used for the phase fitting analysis (note that even a peak misidentification in the first *XMM-Newton* data set would not affect the glitch parameters or the postglitch phase-coherent solution). We consider two possibilities for the glitch phenomenology. First, given its large amplitude, the exponential term is assumed to amount to essentially the whole spin-up episode, similar to what was observed in the second glitch from 1RXS J170849−400910 (Dall'Osso et al. 2003; Kaspi et al. 2003). This would require that the glitch occurred within an hour from the first *Swift* observation. Alternatively, there could be a residual component of the spin-up that is recovered over a much longer timescale (of the

TABLE 2
PPS Analysis of *Chandra* Data for CXOU J164710.2–455216

Spectral Parameter	Pulse Phase Interval			
	A	B (Minima)	C	D (Maxima)
N_H (cm^{-2})	Fixed at phase-averaged value of 1.9	Fixed at phase-averaged value of 1.9	Fixed at phase-averaged value of 1.9	Fixed at phase-averaged value of 1.9
kT_{BB} (keV)	0.50 ± 0.02	<0.15	0.65 ± 0.15	0.54 ± 0.02
R_{BB} (km at 5 kpc)	0.4 ± 0.1	<20	0.2 ± 0.1	0.44 ± 0.06
PL Γ	Fixed at phase-averaged value of 3.5	Fixed at phase-averaged value of 3.5	Fixed at phase-averaged value of 3.5	Fixed at phase-averaged value of 3.5
F_{BB} (10^{-13} erg cm^{-2} s^{-1})	1.18 ± 0.18	<0.07	0.17 ± 0.03	2.41 ± 0.36
χ^2_ν	0.9 by fitting the four spectra together	0.9 by fitting the four spectra together	0.9 by fitting the four spectra together	0.9 by fitting the four spectra together

order of months). A behavior of this type was found in the glitch from 1E 2259+586 (Woods et al. 2004), where the exponential recovery amounted to just ~25% of the whole spin-up. In our coherent postglitch timing solution, a residual spin-up component would imply a negative linear trend in the preglitch phases. The *XMM-Newton* data point could thus be in the position reported in Figure 4 or shifted by multiples of 2π.

Another possibility is that the exponential did not start exactly at t_0, as it would have if the exponential had a finite rise time, or the glitch did not occur at exactly the same time as the burst. We found that even a delay of 8 hr (0.33 days) would decrease the expected value of the residual component of the spin-up by less than a factor of 2. Note that the 8 hr delay corresponds to the uncertainty in the glitch epoch determination of Woods et al. (2004) in the case of 1E 2259+586.

As a last step, we disregarded our identification of the peaks, based on the requirement that two (out of the three) peaks remain nearly constant in relative phase and amplitude (see above) and looked for further possible timing solutions by selecting the other two peaks as the initial reference peak. The result of this additional analysis is reported in Figure 5, where the best possible alternative solution is shown. This was obtained by choosing the highest peak for each folded light curve and/or the nearest peak to the phase extrapolation of the possible timing solution. Fitting these phases with a model which included a $\dot{P}$ component gave a reduced χ^2 of 2.5 (for 11 dof) corresponding to $P = 10.610654(1)$ s and $\dot{P} = 1.66(57) \times 10^{-12}$ s s^{-1} (the values are very close to those reported by Woods et al. 2006). The first 3–4 data points display a marked scattering and give the largest contribution of the high χ^2 value quoted above. Moreover, the phase of the first *XMM-Newton*

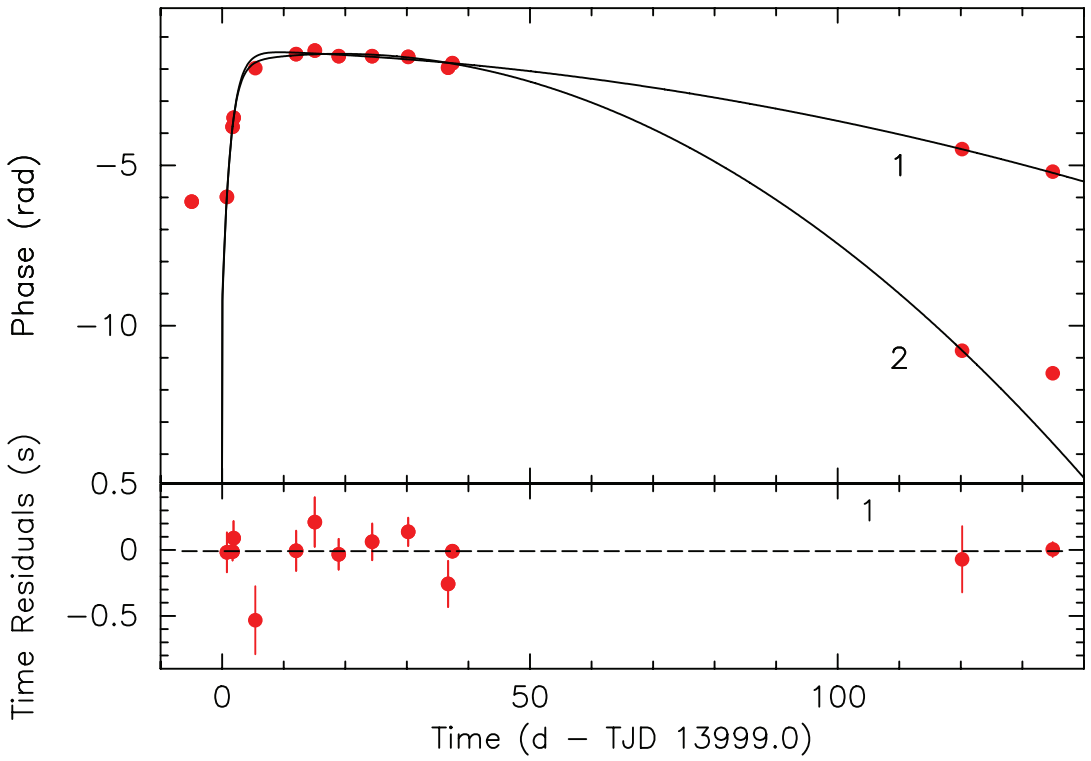

Fig. 4.—Phases (*top*) of the *Swift* XRT, *XMM-Newton* and *Chandra* observations of CXOU J164710.2–455216 (see the text for the discussion concerning the *XMM-Newton* preburst phase position): a large and quick decaying component is clearly present. Time residuals (*bottom*) in seconds of the above datapoints with respect to the phase-coherent *P*-$\dot{P}$ timing solution discussed in the text and including an exponential component. Note that the first *XMM-Newton* point (at day −5) would be at the reported phase only in the hypothesis where the pre- and postglitch parameters are similar (see the text for discussion).

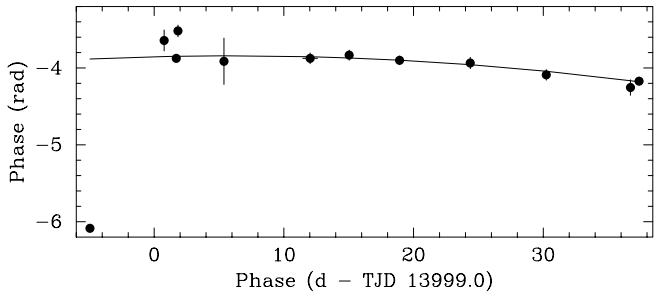

FIG. 5.—Best alternative solution we found by removing our initial hypothesis of having two peaks nearly constant through all the observations (see the text for details). Superimposed is the fitted model including a linear and quadratic term (without considering the preburst *XMM-Newton* observation).

pointing (even assuming a displacement of 2π in the y-axis position) would be too far to be reconciled with any simple timing solution involving only a P and $\dot{P}$ component. We therefore regard this possibility as highly unlikely.

By means of the timing solution reported above, we folded the *Swift* XRT light curves in 13 phase bins and inferred the corresponding root mean square (rms) pulsed fraction for each of them. In Figure 6 (*bottom*) we report both the rms pulsed fraction as well as the pulsed intensity (in counts per second) as a function of the average source intensity. The fractional rms rose toward the pre-outburst value of 0.54 toward the end of the monitoring observations. However, the count rate of the pulsed component remained

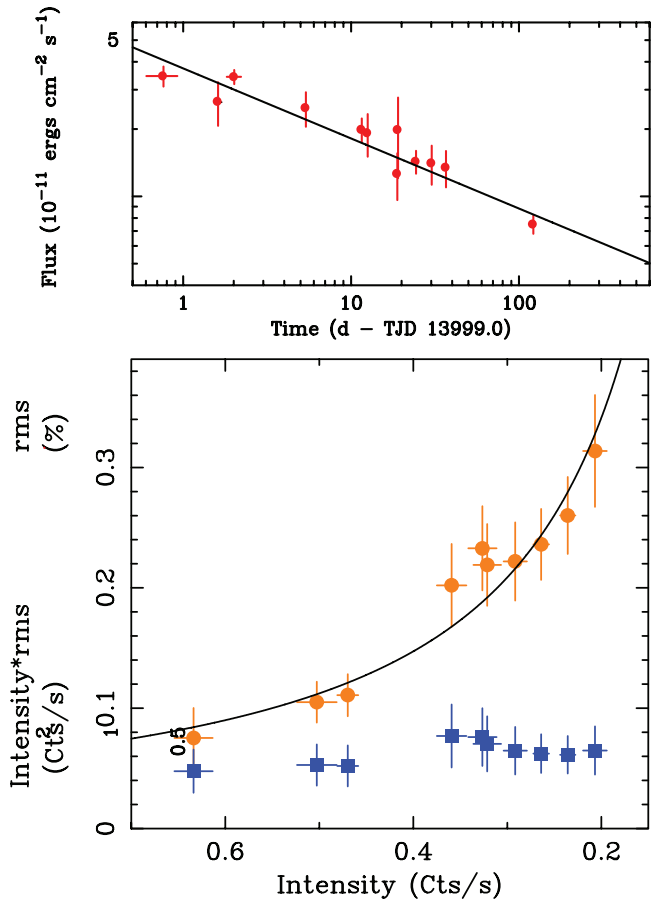

FIG. 6.—The 1–10 keV *Swift* XRT flux light curve of CXOU J164710.2−455216 with the power-law component superimposed used to model the decay (*top*; see text for details). The 10.6 s signal fractional rms (*filled circles*) and pulsed intensity (*filled squares*) as a function of the average source count rate (*bottom*).

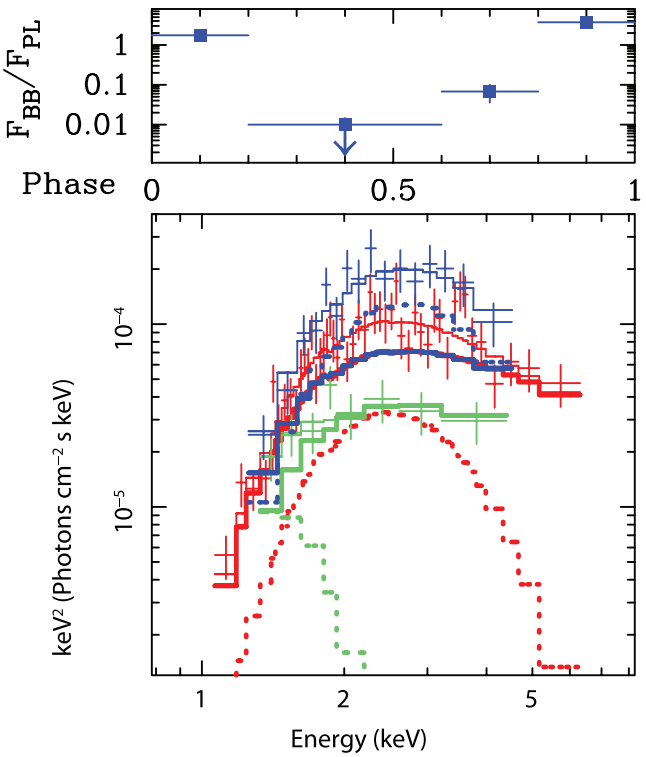

FIG. 7.—ACIS-S *Chandra* Pulse Phase Spectroscopy results (only three phase intervals are reported for clarity) obtained from archival *Chandra* data of CXOU J164710.2−455216 by assuming a BB-plus-PL spectral model. The BB components are marked by the dotted lines, PL with the solid ones. The flux ratio of the two components is also shown in the top panel as a function of pulse phase.

nearly constant throughout the outburst, despite a factor of ≈3 variation in the average flux.

A search both in XRT and BAT monitoring data for additional X-ray bursts like the one detected by BAT gave negative results.

2.3. *Chandra Archival Data Sets*

We retrieved from the *Chandra* archive two observations of Westerlund 1 carried out with the ACIS-S imaging array on 2005 May 22–23 and 2005 June 18–19 with effective exposure time of 18.8 and 38.5 ks, respectively. The observations were obtained in faint-event mode using a 3.2 s frame time. Details on the reduction were reported in Muno et al. (2007) and Skinner et al. (2006). In our re-analysis we focused on a pulse phase-resolved spectroscopy study of the longest observation.

Source photon arrival times were extracted from circular regions with a radius of 2″, which included about 95% of the source photons, and were corrected to the barycenter of the solar system. The best period of the longest observation was determined to be 10.61068(11) s, by fitting the phases of the modulation obtained over 4 consecutive intervals each $\sim 10^4$ s long duration (uncertainties are at the 90% confidence level). The value was consistent with the period reported by Muno et al. (2006b).

By folding the light curve at the best period reported above, a nearly sinusoidal shape of the modulation was found with a large pulsed fraction (∼78% ± 4%; semiamplitude of the modulation divided by the mean source count rate; 52% in term of fractional rms). Moreover, the pulsed fraction was consistent with being slightly energy dependent in the soft and hard bands (pulsed fractions of 70% ± 5%, 88% ± 5% for the 0.5–2 and 2–10 keV bands, respectively; 50% ± 7% and 59% ± 7% in terms of fractional rms). There were also indications that the minimum of the

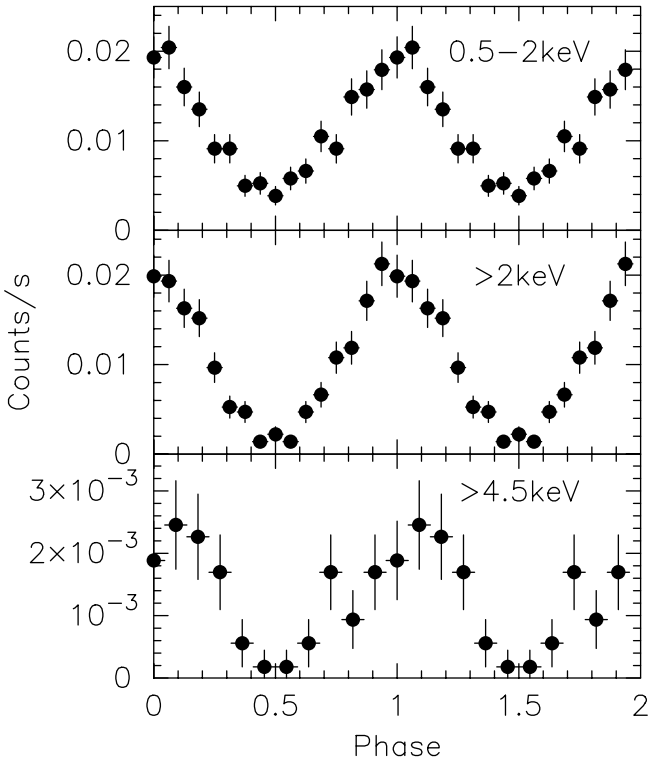

FIG. 8.—The 0.5–10 keV *Chandra* ACIS-S folded light curves at different energies of CXOU J164710.2−455216. Phase 0 is arbitrarily set to TJD 13539.0.

modulation was shallower at high energies (see Fig. 8). Then, we identified four phase intervals (0.0–0.2, 0.2–0.6, 0.6–0.8, and 0.8–1.0; see Figs. 7 and 8), within which a single spectrum was obtained.

We fitted the 1–10 keV phase-averaged spectrum with the BB and BB-plus-PL models. The inclusion of the PL component was found to be significant at the 98% confidence level. The best fit (reduced $\chi^2 \sim 1.14$ for 43 dof) was obtained for $\Gamma = 3.5^{+1.3}_{-0.3}$, $kT \sim 0.49 \pm 0.1$ keV and $R_{\rm BB} \sim 0.4$ km. The PL component accounted for 60% of the total flux. These results are similar to those reported by Skinner et al. (2006). It should be noted, however, that a BB spectrum might not necessarily be the most appropriate description of the spectrum. Indeed, magnetized light-element atmospheres are often used to fit the spectra of magnetic neutron stars. Furthermore, general relativistic corrections (which are not accounted for in the BB model) also play a role in the observed spectrum. In the case of CXOU J164710.2−455216, fits using a magnetized atmosphere and the appropriate general relativistic corrections were reported by Skinner et al. (2006). These yielded a slightly lower effective temperature and a slightly larger radius of the emitting region. However, the statistics were not sufficient to favor this model over the simple BB.

Finally, we carried out phase-resolved spectroscopic by keeping $N_{\rm H}$ and Γ fixed at the values inferred in the phase-averaged spectrum. The results of the spectral fitting are reported in Table 2 and shown in Figure 7 (*bottom*). An *F*-test gave a probability of 99.2% for the PL component to be significant in the four phase interval spectra together. Based on the above analyses, we note that the presence of the PL component was corroborated by the fact that the count rate ratio between the pulse minimum and maximum were approximately equal to the BB/PL flux ratios inferred from the pulse phase spectroscopy analysis (see Figs. 7 and 8). To further test this hypothesis we folded the light curve considering only photons at energies above 4.5 keV, where the contribution from the BB component was negligible at pulse minimum. The shape of the modulation changed drastically with respect to that at lower energies, showing an asymmetric profile with a flat 0.2 phase-long minimum consistent with zero count rate (see Fig. 8).

We note that the unusually small size inferred for the BB emitting region (radius of 270 m) is consistent with the large pulsed flux. The BB component is emitted from a hot spot on the neutron star's surface, and the pulsed fraction reaches its minimum as the BB emitting region gets completely occulted for a portion of the star rotation period. Therefore, at pulse minimum, the spectrum is dominated by the PL component.

3. DISCUSSION

In the following we compare the *Swift* results of CXOU J164710.2−455216 with those of other AXPs that showed a similar behavior.

A large glitch ($\Delta\nu/\nu \sim 4 \times 10^{-6}$) was detected from 1E 2259+586, nearly simultaneously with several intense (total fluence of $\sim 3 \times 10^{-8}$ erg cm^{-2}) and short SGR-like bursts (Woods et al. 2004; Kaspi et al. 2003). Our *Swift* and *XMM-Newton* coherent timing solution of CXOU J164710.2−455216 implies that an even larger glitch ($\Delta\nu/\nu = 6.5 \times 10^{-5}$) occurred within 0.8 days of the burst epoch. The glitch was more than 1 order of magnitude larger than previous glitches detected from AXPs, or any other type of pulsar. This holds true even considering the minimum value of the residual component of the spin-up for a possible long-term glitch recovery component. The glitch effects ($\Delta\nu/\nu \approx 6 \times 10^{-5}$) were recovered for the most part over less than 2 days, although the exponential component was still detectable after 1 week. In this respect the exponential decay time and its amplitude are, taken separately, within the wide range found for radio pulsars, but they were never observed to occur together (Wong et al. 2001; Hobbs et al. 2002). On the other hand, the combination of quick recovery and large amplitude is similar to that observed in other AXPs/SGRs (Dall'Osso et al. 2003; Woods et al. 2004). We also detected a secular spin-down $\dot{P} = 9.2(4) \times 10^{-13}$ s s^{-1}, implying a dipole field strength of $\simeq 1 \times 10^{14}$ G (assuming a neutron star radius of 10 km and a mass of 1.4 $M_\odot$), a value not dissimilar to that inferred for other AXPs. The long-term recovery of the glitch can be reasonably expected to be characterized by a second derivative of the period, which might be revealed by future monitoring observations of the source (as in the case of 1RXS J170849−400910, where it was revealed over a ~500 day timescale). The detection of such a component would provide a further confirmation of the presence and amplitude of the residual component, especially once the recovery timescale is known (cf. Dall'Osso et al. 2003, § 6.3 and references therein). From the energetic point of view we note that whatever was the cause of the burst, the glitch, and the outburst, it released approximately 5×10^{41} erg during the first 130 days, 0.004% of which was emitted during the burst; 6% was stored in the star during the glitch and lost again (either through internal dissipation or emission) within a couple of days. More than 90% of the total went to increase the persistent (mostly unpulsed) emission. Future monitoring observations of the source flux decay until the quiescence level will allow us to quantify the total energy budget of the outburst.

The prompt X-ray afterburst properties of CXOU J164710.2−455216 are also amazingly similar to those of 1E 2259+586. In fact, in the case of 1E 2259+586, a drop in the pulsed fraction was observed together with a change in the pulse shape (from 25% to 15% rms) quickly recovering (within a week) toward the preburst shape and pulsed fraction. Similarly, the CXOU J164710.2−455216 pulse shape varied from a nearly sinusoidal shape (before the burst) to a double-peaked one (after 1 day) and

to a triple-peak shape (for epochs later than 2 days), while the pulsed fraction dropped from a value of ~80% (as recorded by an *XMM-Newton* observation few days before the burst) to ~10% few hours after the BAT event. Since then the pulsed fraction has been recovering toward its preburst value. Moreover, the flux decay of CXOU J164710.2−455216 is reminiscent of that of 1E 2259+586, e.g., a power law $F \propto t^{\alpha}$, with α index of -0.28 ± 0.05 after the first day from the BAT event (compared with the -0.22 in 1E 2259+586). It is also apparent that the PL component decayed more rapidly (α index of -0.38 ± 0.11; 90% uncertainty) than the BB flux (α index of -0.14 ± 0.10). This implies that the cooling timescale of the hot spots on the neutron star's surface is longer than that of the region responsible for the PL, likely an active coronal region (used to account for the broadband nonthermal PL component; Beloborodov & Thompson 2007). Regardless of the scenario, the pulsed emission was mainly accounted for by the BB, and the increase of the pulsed fraction in the postburst phases was caused by the increase in the fractional contribution of the BB flux as the nearly unpulsed PL component decayed. Further evidence in favor of this comes from the rise in the fractional rms as a function of time. This was well fitted by a power law with index α of $+0.38 \pm 0.11$, which is opposite to the slope of the decay of the amplitude of the power-law component.

The BB component also appears to play an important role in the quiescent state of this AXP, as shown by our PPS study in § 2.3, where the timing and spectral properties were found to be consistent with the 100% pulsed component being totally accounted for by the BB component. This very high degree of modulation is consistent with the small size of the region for the BB component, if this originates at the NS surface and is periodically self-eclipsed by rotation. For a typical star of radius ~10 km, and a distance of ~5 kpc, the angular size BB emitting spot is only a few degrees. Although light-bending effects contribute to substantially suppress the degree of modulation, for a spot of such a small extent there exist geometries for which complete occultation can be achieved for a part of the star rotation (Pechenick et al. 1983; see also Riffert & Meszaros 1988 and Özel 2002; DeDeo et al. 2001).

It is interesting to note that, although formally not required from a statistically point of view, there were indications of the presence of a soft excess in the *Chandra* spectrum corresponding to the pulse minimum (where the BB from the hot spot is absent; see Fig. 7, *bottom*). By modeling this excess with a BB component we obtained an upper limit of $kT \leq 0.15$ keV and radius consistent with the NS size. If confirmed by future observations of CXOU J164710.2−455216 in quiescence, this latter component might provide evidence for the thermal radiation emitted from the whole NS surface (similar to what we observed in the quiescent spectrum of XTE J1810−197).

One of the main differences between the outbursts from CXOU J164710.2−455216 and 1E 2259+586 is that the quiescent flux component was a factor of 100 larger in 1E 2259+586, so that the relative amplitude of the outburst was smaller. In fact, the luminosity of these two sources one day after their respective glitches were the same to within a factor of 2 (1E 2259+586 was slightly brighter). In this respect, the outburst properties of the two AXPs are more similar than they would appear at first sight. Indeed, the longer timescales over which the pulsed component rms recovers its initial value in CXOU J164710.2−455216 is likely due to the fainter quiescent level of this source with respect to that in 1E 2259+586 (where the rms is completely recovered, i.e., it reaches the pre-outburst value, in less than a week).

Particularly interesting is the event detected in 2003 from another historical AXP, namely 1E 1048.1−5937. A clear anticorrelation between pulsed fraction and intensity of the source was detected and found to be accompanied by relatively small variations in the phase-averaged spectrum (Tiengo et al. 2005). The presence of a hard component was detected in the PPS study at the maximum of the pulses. A monitoring campaign of 1E 1048.1−5937 carried out by RXTE showed that this phenomenology was also accompanied by a large outburst of the source flux above its previous average value, which lasted for about 2 yr. However, no burst was detected close to the outburst onset epoch (Kaspi et al. 2006). In this case the timescale over which the pulsed fraction was recovered was of the order of the outburst duration itself instead of 1 week (as observed in 1E 2259+586). This event has several similarities with the one currently observed in CXOU J164710.2−455216.

Finally, it is premature to draw similarities between the outbursting behavior of CXOU J164710.2−455216 during the first month and that of XTE J1810−197, (Ibrahim et al. 2004; Gotthelf et al. 2004; Israel et al. 2004; Rea et al. 2004). Both the timing and spectral properties appear to be different; the pulsed fraction of XTE J1810−197 increased its value from a pre-outburst upper limit of 20% (in the 0.1–2.5 keV band) to a 1–10 keV measurement of ~53% after about 1 yr, and decreased since then. Moreover, the quiescent spectrum differed, in that it was dominated by a very soft and extended BB in XTE J1810−197 and by a relatively hard and especially small radius BB in CXOU J164710.2−455216. These differences may result from different viewing angles of and/or different burst emitting regions.

4. CONCLUSIONS

On 2006 September 21, the candidate AXP CXOU J164710.2−455216 emitted a short and rather intense burst that was promptly detected by the *Swift* BAT. Together with the burst, large changes in the timing and spectral properties of the persistent component were detected and seen evolving during the subsequent weeks. In particular, the *Swift* XRT monitoring (plus two proprietary *XMM-Newton* and two archival *Chandra* observations) allowed us to find the following.

1. The pulse phase evolution is consistent with the occurrence of a large glitch ($\Delta\nu/\nu \sim 10^{-4}$), the largest ever detected from a neutron star. The glitch was recovered over a timescale of 1.4 days, although its effects were present in the pulse phases until approximately 1 week after the glitch epoch. We also detected a quadratic component in the pulse phases corresponding to a $\dot{P} = 9.2(4) \times 10^{-13}$ s s^{-1}.

2. The first 1–10 keV *Swift* XRT spectrum was measured ~13 hr after the burst detection and showed, in addition to a $kT \sim 0.65$ keV blackbody ($R_{\rm BB} \sim 1.5$ km), a $\Gamma \sim 2.3$ power-law component accounting for about 50% of the observed flux.

3. The flux decay of CXOU J164710.2−455216 is well described by the function $F \propto t^{\alpha}$, with index α of -0.28 ± 0.05 (similar to the case of the 2002 1E 2259+586 burst-active phase). Moreover, we found that the PL component decays more rapidly (index α of -0.38 ± 0.11; 90% uncertainty) than the BB flux (index α of -0.14 ± 0.10).

4. The pulsed fraction of the 10.61 s pulsations was seen to drop from a value of ~80% (as recorded by an *XMM-Newton* observation a few days before the burst) to ~10% a few hours after the BAT event. The spectral and timing analysis clearly show that only the blackbody component is responsible for the pulsed flux (at least during the initial phases of the outburst).

5. Archival *Chandra* data analysis revealed that the modulation in quiescence is 100% pulsed at energies above ~4 keV and consistent with the (unusually small-sized) blackbody component being occulted by the neutron star as it rotates.

6. A comparison of the properties of CXOU J164710.2−455216 with those of other AXPs which showed similar behavior confirmed that outbursting events of this kind are more common than previously thought.

All these results confirmed unambiguously that CXOU J164710.2−455216 is a transient and bursting AXP, showing an unusually high pulsed fraction level in quiescence. Studying how the source will return from its postburst/glitch timing and spectral properties to the quiescent ones might help reveal the mechanisms behind the outbursts of AXPs. Finally, the BAT detection of bursts from CXOU J164710.2−455216 opens a new perspective for detecting bursts from known AXPs, and for identifying new AXPs/SGRs with *Swift*.

This work is partially supported at OAR through Agenzia Spaziale Italiana (ASI), Ministero dell'Istruzione, Università e Ricerca Scientifica e Tecnologica (MIUR-COFIN), and Istituto Nazionale di Astrofisica (INAF) grants. We acknowledge financial contribution from contract ASI-INAF I/023/05/0. We thank Neil Gehrels for approving the *Swift* ToO observation program and Norbert Schartel for approving the *XMM-Newton* postburst observation through the Director's Discretionary Time program. We thank Patrizia Romano for her help in the quick look of the TDRSS data of the BAT event. We also thank Nanda Rea, Andrea Possenti, Marta Burgay, Diego Götz, and Peter Woods for useful discussions.

Facilities: Swift (BAT), Swift (XRT), CXO (ACIS-S), XMM (EPN)

REFERENCES

Beloborodov, A. M., & Thompson, C. 2007, ApJ, 657, 967
Burgay, M., Rea, N., Israel, G. L., & Possenti, A. 2006, ATel, 903
Camilo, F., Ransom, S. M., Halpern, J. P., Reynolds, J., Helfand, D. J., Zimmerman, N., & Sarkissian, J. 2006, Nature, 442, 892
Campana, S., & Israel, G. L. 2006, ATel, 893
Cusumano, G., et al. 2005, Proc. SPIE, 5898, 377
Dall'Osso, S., Israel, G. L., Stella, L., Possenti, A., & Perozzi, E. 2003, ApJ, 599, 485
DeDeo, S., Psaltis, D., & Narayan, R. 2001, ApJ, 559, 346
Duncan, R. C., & Thompson, C. 1992, ApJ, 392, L9
Gavriil, F. P., Kaspi, V. M., & Woods, P. M. 2002, Nature, 419, 142
———. 2004, ApJ, 607, 959
Gotthelf, E. V., Halpern, J. P., Buxton, M., & Bailyn, C. 2004, ApJ, 605, 368
Gotz, D., et al. 2006, ATel, 953
Hill, J. E., et al. 2004, Proc. SPIE, 5165, 217
Hobbs, G., et al. 2002, MNRAS, 333, L7
Ibrahim, A. I., et al. 2004, ApJ, 609, L21
Israel, G. L., & Campana, S. 2006, ATel, 896
Israel, G. L., Dall'Osso, S., Campana, S., Muno, M., & Stella, L. 2006, ATel, 932
Israel, G. L., & Stella, L. 1996, ApJ, 468, 369
Israel, G. L., et al. 2004, ApJ, 603, L97
Kaspi, V. 2006, in Isolated Neutron Stars: From the Interior to the Surface, ed. S. Zane, R. Turolla, & D. Page (Astrophysics & Space Science), in press (astro-ph/0610304)
Kaspi, V., Dib, R., & Gavriil, F. 2006, ATel, 794, 1
Kaspi, V. M., Gavriil, F. P., Woods, P. M., Jensen, J. B., Roberts, M. S. E., & Chakrabarty, D. 2003, ApJ, 588, L93
Krimm, H., Barthelmy, S., Campana, S., Cummings, J., Israel, G., Palmer, D., & Parsons, A. 2006, GCN Circular 5581
Mereghetti, S., & Stella, L. 1995, ApJ, 442, L17
Muno, M., Gaensler, B., Clark, J. S., Portegies Zwart, S., Pooley, D., de Grijs, R., Stevens, I., & Negueruela, I. 2006a, ATel, 902
Muno, M. P., et al. 2007, ApJ, submitted
———. 2006b, ApJ, 636, L41
Özel, F. 2002, ApJ, 575, 397
Paczyński, B. 1992, Acta Astron., 42, 145
Pechenick, K. R., Ftaclas, C., & Cohen, J. M. 1983, ApJ, 274, 846
Rea, N., Tiengo, A., Mereghetti, S., Israel, G. L., Zane, S., Turolla, R., & Stella, L. 2005, ApJ, 627, L133
Rea, N., et al. 2004, A&A, 425, L5
Riffert, H., & Meszaros, P. 1988, ApJ, 325, 207
Skinner, S. L., Perna, R., & Zhekov, S. A. 2006, ApJ, 653, 587
Thompson, C., & Duncan, R. C. 1995, MNRAS, 275, 255
Tiengo, A., Mereghetti, S., Turolla, R., Zane, S., Rea, N., Stella, L., & Israel, G. L. 2005, A&A, 437, 997
Wang, Z., Kaspi, V. M., Osip, D., Morrell, N., Kaplan, D. L., & Chakrabarty, D. 2006, ATel, 910
Wong, T., Backer, D. C., & Lyne, A. G. 2001, ApJ, 548, 447
Woods, P., & Thompson, C. 2004, in Compact Stellar X-ray Sources, ed. W. H. G. Lewin & M. van der Klis (Cambridge: Cambridge Univ. Press), 547
Woods, P. M., Kaspi, V. M., & Gavriil, F. 2006, ATel, 929
Woods, P. M., et al. 2004, ApJ, 605, 378
———. 2005, ApJ, 629, 985